

Supplementary Information

Interaction between Bile Salt Sodium Glycodeoxycholate and PEO-PPO-PEO Triblock Copolymers in Aqueous Solution

Solmaz Bayati,¹ Caroline Anderberg Haglund,^{1,§} Nicolae V. Pavel,² Luciano Galantini,² and Karin Schillén^{1,*}

¹ *Division of Physical Chemistry, Department of Chemistry, Lund University, P.O. Box 124, SE-221 00 Lund, Sweden*

² *Department of Chemistry, "Sapienza" University of Rome, P. le A. Moro 5, 00185 Rome, Italy*

[§] *Current address: AkzoNobel Industrial Coatings AB, Staffanstorpsvägen 50, SE-205 17 Malmö, Sweden*

Corresponding Author. *E-mail: Karin.Schillen@fkem1.lu.se.

Self-Association of P65 Copolymer in Water

Differential Scanning Calorimetry

Table S1. Calorimetric data for 0.5 – 10.0 wt % P65 in water.

P65 wt %	P65 mM	T_m °C	T_{onset} °C	ΔH_{tr} kJ/mol polymer	ΔH_{tr} kJ/mol PO
0.499	1.47	47.3	40.1	82	2.8
1.00	2.94	43.7	38.1	81	2.8
2.50	7.35	40.4	34.9	106	3.7
5.00	14.7	37.2	32.4	106	3.7
10.0	29.4	34.0	28.9	122	4.2

Dynamic and Static Light Scattering

Figure S1a presents the pseudo-cross intensity correlation functions $g^{(2)}(t) - 1$ of a solution of 1.0 wt % P65 in water as a function of temperature. The corresponding relaxation time distributions obtained by regularized inverse Laplace transformation is displayed in Figure S1b. The fast and a slow relaxation mode in the distribution at 20 °C were assigned to the single block copolymer chains (unimers) and clusters of hydrophobic contaminants.¹⁻² The third small intermediate mode that appeared at 30 °C was connected to P65 micelles.

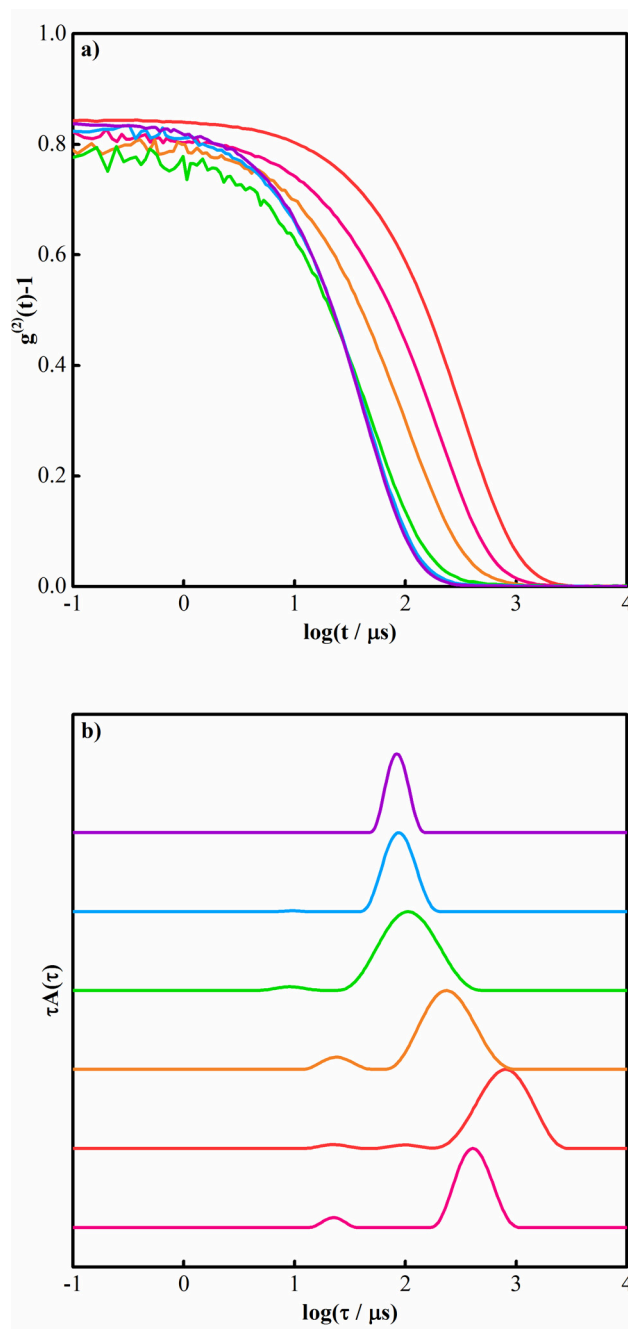


Figure S1. DLS data of 1.0 wt % P65 in water. a) Pseudocross intensity correlation functions at 20 °C (pink), 30 °C (red), 35 °C (orange), 40 °C (green), 45 °C (blue) and 50 °C (violet.) b) Corresponding relaxation time distributions (normalized by height) with the same color code as in a). Both data sets were shifted by a factor $\log(T\eta_{293}/293\eta_T)$ on the x-axis, i.e. relative to the 20 °C data.

The temperature dependence of the total Rayleigh ratio at the scattering angle $\theta = 90^\circ$ ($R_{\theta=90}$) of a 1.0-wt% P65 solution is presented in Figure S2. At low temperature, where the solution consisted of soluble P65 chains (unimers) (see the DSC results in Figure 1 in the article and Table S1 above), the scattering intensity was low whereafter it sharply increased as an indication of the formation of micelles. The CMT was estimated to be 40 °C from the breakpoint in the curve.

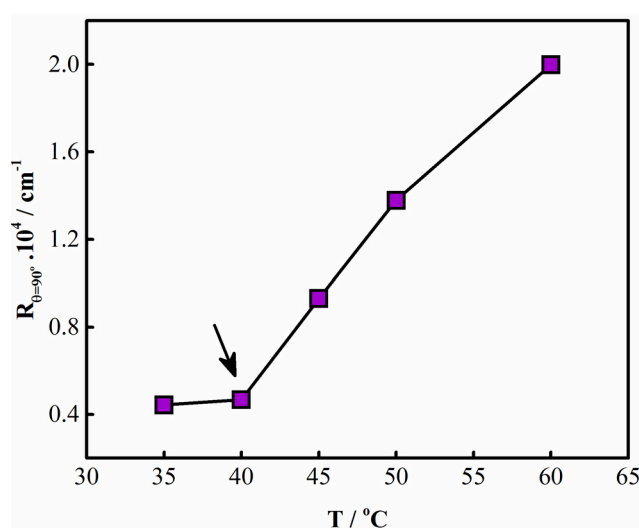


Figure S2. Total Rayleigh ratio (without subtraction of the solvent scattering intensity) measured at scattering angle $\theta = 90^\circ$ for a 1.0-wt % P65 aqueous solution as a function of temperature. The arrow indicates the critical micelle temperature. The solid line is a guide to the eye.

Effect of NaGDC on the Self-Association of P65 and F127

Differential Scanning Calorimetry

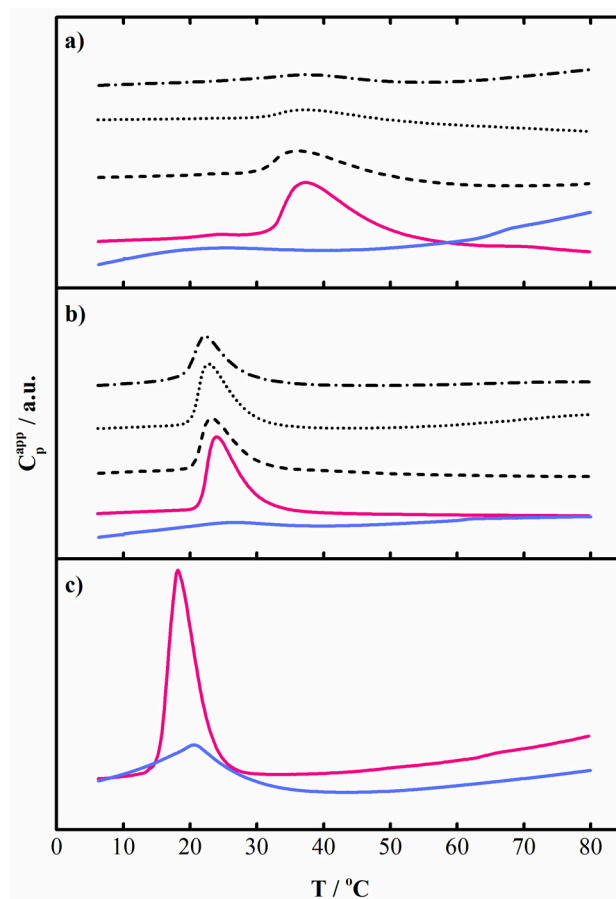


Figure S3. DSC thermograms for PEO-PPO-PEO block copolymer–NaGDC solutions at various molar ratios, $MR = n_{NaGDC}/n_{polymer}$. (a) P65–NaGDC solutions, (b) F127–NaGDC solutions and (c) P123–NaGDC solutions. MR = 0 (pink), MR = 0.3 (dashed line), MR = 0.6 (dotted line), MR = 3 (dashed dotted line) and MR = 12 (blue). The block copolymer concentration was 5.0 wt %.

Table S2. Calorimetric data for 1.0-wt % P65 solution with different NaGDC concentrations.

P65 wt %	mM	NaGDC mM	NaGDC/P65 molar ratio	T_m °C	T_{onset} °C	ΔH_{tr} kJ/mol polymer	ΔH_{tr} kJ/mol PO
1.00	2.94	0	0	43.7	38.1	81	2.8
0.998	2.93	0.942	0.32	40.7	33.9	128	4.4
0.999	2.94	1.66	0.57	40.5	33.8	68	2.4
0.999	2.94	8.36	2.8	41.3	33.3	38	1.3

Table S3. Calorimetric data for 5.0-wt % P65 solution with different NaGDC concentrations.

P65 wt %	mM	NaGDC mM	NaGDC/P65 molar ratio	T_m °C	T_{onset} °C	ΔH_{tr} kJ/mol polymer	ΔH_{tr} kJ/mol PO
5.00	14.7	0	0	37.2	32.4	106	3.7
5.00	14.7	4.72	0.32	36.5	30.1	61	2.1
4.99	14.7	8.31	0.57	37.4	31.0	19	0.7
4.98	14.6	41.7	2.8	38.6	26.2	21	0.7
5.00	14.7	176.3	12.0	–	–	–	–

Table S4. Calorimetric data for 1.0-wt % F127 solution with different NaGDC concentrations.

F127 wt %	mM	NaGDC mM	NaGDC/F127 molar ratio	T_m °C	T_{onset} °C	ΔH_{tr} kJ/mol polymer	ΔH_{tr} kJ/mol PO
0.998	0.792	0	0	27.6	25.3	310	4.6
0.998	0.792	0.231	0.29	27.4	24.8	310	4.6
0.997	0.791	0.447	0.56	27.3	24.5	305	4.5
0.995	0.790	2.29	2.9	26.5	23.9	247	3.6
1.000	0.793	9.57	12.1	31.0	24.1	79.3	1.2

Table S5. Calorimetric data for 5.0-wt % F127 solution with different NaGDC concentrations.

F127 wt %	F127 mM	NaGDC mM	NaGDC/F127 molar ratio	T_m °C	T_{onset} °C	ΔH_{tr} kJ/mol polymer	ΔH_{tr} kJ/mol PO
4.99	3.96	0	0	24.0	21.5	315	4.6
5.00	3.97	1.16	0.29	23.3	20.5	233	3.4
4.99	3.96	2.24	0.56	22.7	20.2	275	4.0
5.01	3.97	11.5	2.9	22.2	19.4	184	2.7
4.99	3.96	47.5	12.1	–	–	–	–

Dynamic Light Scattering

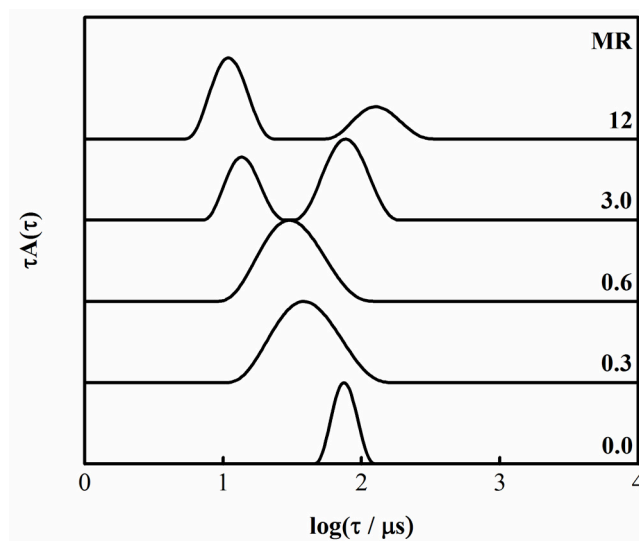


Figure S4. Relaxation time distributions of P65-NaGDC mixed solutions with molar ratios (MR = $n_{\text{NaGDC}}/n_{\text{P65}}$) as indicated at 50 °C. The P65 concentration was 5.0 wt %.

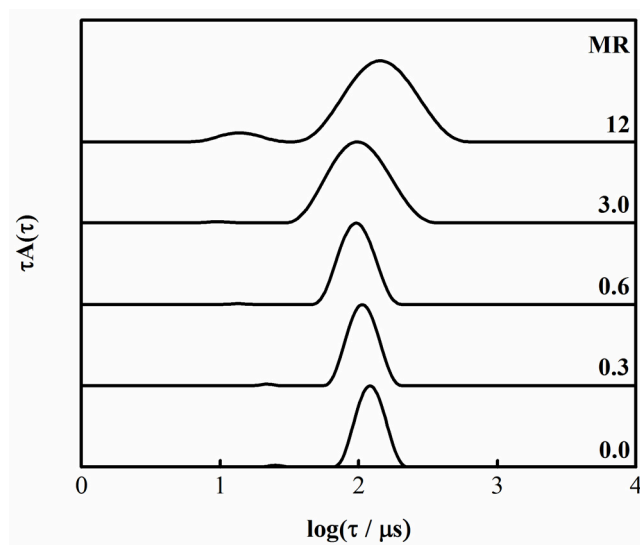


Figure S5. Relaxation time distributions of F127-NaGDC mixed solutions with molar ratios ($\text{MR} = n_{\text{NaGDC}}/n_{\text{F127}}$) as indicated at 50 °C. The F127 concentration was 5.0 wt %.

Small Angle X-ray Scattering

Table S6. Results from fitting of SAXS data for P65 in water and for aqueous mixed P65–NaGDC solutions at different molar ratios, MR. The temperature was 50 °C and the P65 concentration was 5.0 wt %.

MR ^a	0	0.30	0.60	3.0	12.0
fitting model	spherical core-shell	spherical core-shell	spherical core-shell	<i>not analyzed</i>	sphere
$S(q)$ model	Percus-Yevick	Hayter-Penfold	Hayter-Penfold		Hayter-Penfold
χ^2	2.1	2.2	5.1		3.8
$bk g^b \cdot 10^4 / \text{cm}^{-1}$	15.4±0.2	16.6±0.0	6.7±0.0		40.3±0.2
charge	–	11.75±0.06	23.1±0.1		18.12±0.05
$\rho_{core}^c \cdot 10^6 / \text{\AA}^{-2}$	9.3428±0.004	9.3779±0.005	9.3736±0.007		10.136±0.002
ϵ^d	–	69.9	69.9		69.9
R_{core}^e / nm	3.47±0.01	3.140±0.003	2.833±0.003		1.984±0.002
C_{salt}^f / mM	0	1.69	3.47		–
scale factor	1	1	1		1
$\rho_{shell}^g \cdot 10^6 / \text{\AA}^{-2}$	9.661±0.002	9.729±0.003	10.086±0.002		–
$\rho_0^h \cdot 10^6 / \text{\AA}^{-2}$	9.3065	9.3065	9.3065		9.3065
d_{shell}^i / nm	1.91±0.02	1.763±0.002	1.163±0.003		–
ϕ^j	0.0872	0.0659	0.0356		0.10093
$PD^k R_{core}$	0.12	0.12	0.19		–
$PD^k d_{shell}$	0.03	0.11	0.05		–
$PD^k R_{tot}$					0.25
R_{tot}^l / nm	5.384±0.02	4.903±0.003	3.996±0.004		1.984±0.002

^a $n_{\text{NaGDC}}/n_{\text{polymer}}$ molar ratio, ^b background, ^c X-ray scattering length density of the core, ^d dielectric constant of the solvent, ^e core radius, ^f salt concentration, ^g X-ray scattering length density of the shell, ^h X-ray scattering length density of H₂O, ⁱ shell thickness, ^j volume fraction, ^k polydispersity (Schulz model), ^l total radius (errors estimated from the errors in values of the core and corona radii). The errors correspond to those reported by the SasView software.

EXPERIMENTAL SECTION

Differential Scanning Calorimetry. DSC measurements were performed using a high sensitivity MicroCal™ VP-DSC (Microcal, Northampton, MA). The experimental conditions can be found in refs ³ where a complete information about the instrument is given in addition to that of ref ⁴. Two different sets of DSC experiments were performed, both with a scan rate of 1 °C/min. First, the pure P65 aqueous solutions with concentration in the range of 0.50–10.0 wt % (or 1.47–29.4 mM) were investigated. Thereafter, measurements carried out on mixed block copolymer (P65, F127 or P123)–NaGDC solutions containing 1.0 wt % block copolymer and varying sodium glycodeoxycholate (NaGDC) concentration corresponding to NaGDC/P123 molar ratios ($MR = n_{\text{NaGDC}}/n_{\text{P123}}$): 0.3, 0.6, 3 and 12. The obtained endothermic transition peaks were normalized by the block copolymer concentration and corrected for the base line. The area under the peak gave the enthalpy of transition ΔH_{tr} . The temperature where the transition started, denoted T_{onset} , was obtained from the intersection of the linear extrapolation of the baseline and the peak ascent and the temperature at the peak maximum is denoted T_m .

Dynamic and Static Light Scattering. Dynamic and static light scattering measurements were carried out by means of an ALV/DLS/SLS-5022F, CGF-8F-based compact goniometer (ALV-GmbH, Langen, Germany). A 22 mW He-Ne laser with the wavelength of 632.8 nm was used as the light source. An F32 Julabo heating circulator was used to control the temperature (± 0.01 °C). A more detailed description of the instrument can be found in refs ^{3, 5}. The solutions studied by light scattering were filtered cold into 10-mm clean cylindrical borosilicate glass cells through a sterile 0.20 μm Minisart© filter (Sartorius, Germany) and were equilibrated at the measuring temperature for 30 minutes, prior to the measurement. For

measuring temperatures above room temperature, the solutions were equilibrated for at least 60 minutes at room temperature and thereafter at the measuring temperature for 30 minutes.

In the case of the P65 aqueous solutions, the experiments were carried out at the temperature interval of 20–50 °C. However, for the block copolymer (P65, P123 or F127)–NaGDC mixtures the measurements were performed at 50 °C. DLS and SLS measurements were performed at six scattering angles, θ , in the range of 40–130°. However, since the obtained scattering intensities were angular independent the presented results are only those of $\theta = 90^\circ$.

DLS Data Analysis. The intensity correlation function $g^{(2)}(t)$ was obtained directly from the ALV software in the form of $g^{(2)}(t) - 1$ versus lag time t . The functions were analyzed directly using the constrained nonlinear regularization algorithm Regularized Positive Exponential Sum (REPES) included in the GENDIST software, from which the relaxation time distribution $A(\tau)$ and the relaxation time, τ were obtained.⁶⁻⁷ The distributions in this work are displayed as $\tau A(\tau)$ vs $\log(\tau)$ for equal-area representation.⁸ The apparent hydrodynamic radius, $R_{H,app}$, was calculated from the Stokes-Einstein equation: $R_{H,app} = kT/6\pi\eta_0 D$, where k is the Boltzmann constant, η_0 is the viscosity of the solvent at the absolute temperature T . D is the apparent collective diffusion coefficient, which for translational motion of the scattering particles is defined as

$$D = \lim_{q \rightarrow 0} (\Gamma/q^2) \tag{S1}$$

where $\Gamma = 1/\tau$ is the relaxation rate and q is the magnitude of the scattering vector, which is related to the refractive index of the solvent (n), and the incident light wavelength (λ) as $q = 4\pi n \sin(\theta/2)/\lambda$.

Static Light Scattering. In a SLS measurement, the scattered intensity of a solution of scattering particles may be expressed as the total Rayleigh ratio, R_θ , i.e., without subtraction of the solvent scattering intensity, according to

$$R_\theta = (I_s(\theta)/I_{tol})R_{tol}(n/n_{tol})^2 \quad (S2)$$

where $I_s(\theta)$ is the intensity of scattered light at angle θ , I_{tol} is the scattering intensity of toluene, R_{tol} is the Rayleigh ratio of the toluene at 90° ($1.4206 \cdot 10^{-5} \text{ cm}^{-1}$) and $n_{tol} = 1.496$ is the refractive index of the toluene. In this work, the SLS measurements were performed at $\theta = 90^\circ$.

SAXS Data Analysis. The scattering intensity for a group of n monodisperse spherical particles per unit volume of the medium can be defined as

$$I(q) = \phi V_{tot} P(q) S(q) \quad (S3)$$

where $P(q)$ is the particle form factor, which contains information about the particle size and shape, $S(q)$ is the structure factor, which is linked to the interparticle interactions, V_{tot} is the volume of one particle, ϕ is the volume fraction of the particles, and the number density of particles is given by $n = \phi/V_{tot}$.

The data were treated with two approaches. The first approach was to employ an indirect Fourier transformation method to obtain the pair distance distribution function, $p(r)$. This function contains information about the size and the shape of the scattering particle and is related to the scattering intensity by the equation below

$$I(q) = 4\pi \int_0^\infty p(r) \frac{\sin qr}{qr} dr \quad (S4)$$

This approach was accomplished with the help of “Bayesapp” software developed by Hansen.⁹ By means of this software, $p(r)$ function and the interparticle interaction as an excluded volume distribution could be extracted simultaneously without any priori information about the interparticle interactions.

The second approach was to treat the data based on an appropriate model for the form and the structure factor. By means of SasView software,¹⁰ and depending on the scattering behavior of the particles in the mixed block copolymer–NaGDC solutions, the form factor and the structure factor were treated with one of the following models

1) The Debye model for the flexible polymer chains as $P(q)$ with no structure factor due to the low block copolymer concentration (i.e., $S(q) = 1$) at 20 °C for pure P65 and F127 solutions at MR = 0 as equation below

$$I(q) = scale \times 2 \left[\exp\left(- (qR_g)^2\right) + (qR_g)^2 - 1 \right] / (qR_g)^4 \quad (S5)$$

where $scale$ is the scale factor and R_g is the polymer chain radius of the gyration.

2) The spherical core-shell model as $P(q)$ (Eq S6) together with a $S(q)$ following the Percus-Yevick closure (i.e., a hard sphere structure factor) (Eq S7),¹¹⁻¹² i.e., at MR = 0 for solutions of pure P123 block copolymer at 20 °C, and P65 block copolymer at 50 °C. For block copolymer–NaGDC mixed solutions containing P65 with MR = 0.3-0.6 at 50 °C, the spherical core-shell model as $P(q)$ was used together with a $S(q)$ for a system of charged hard spheres that interact via repulsive screened Coulomb pair potential. $S(q)$ was obtained by following the Hayter-Penfold (HP) model to solve the Ornstein-Zernike equation under the mean spherical approximation.¹³

$$I(q) = n \left[3V_{core}(\rho_{core} - \rho_{shell}) \frac{\sin(qR_{core}) - qR_{core} \cos(qR_{core})}{(qR_{core})^3} + 3V_{tot}(\rho_{shell} - \rho_0) \frac{\sin(qR_{tot}) - qR_{tot} \cos(qR_{tot})}{(qR_{tot})^3} \right]^2 S(q) \quad (S6)$$

where V_{core} is the core volume, ρ_{shell} , ρ_{core} and ρ_0 are the scattering length densities of the shell, the core and the solvent respectively and R_{tot} and R_{core} are the total radius and the core radius of the particle, correspondingly.

$S(q)$ in Eq S6 is described as¹⁴

$$S(q) = \frac{1}{1 + 24\varphi_{HS}G(A)/A}$$

with $A = 2qR_{HS}$

and

$$G(A) = \frac{\alpha(\sin A - A \cos A)}{A^2} + \frac{\beta[2A \sin A + (2 - A^2) \cos A - 2]}{A^3} + \frac{\gamma[-A^4 \cos A + 4((3A^2 - 6) \cos A + (A^3 - 6A) \sin A + 6)]}{A^5}$$

$$\alpha = \frac{(1+2\varphi_{HS})^2}{(1-\varphi_{HS})^4} \quad \beta = \frac{-6\varphi_{HS}(1+\varphi_{HS}/2)^2}{(1-\varphi_{HS})^4} \quad \gamma = \frac{\varphi_{HS}\alpha}{2} \quad (S7)$$

3) homogeneous sphere model as $P(q)$ with the Hayter-Penfold $S(q)$ for 200 mM NaGDC in water at 20 °C and 50 °C as well as P65-, F127- or P123- NaGDC solutions at MR=12 at 20 °C .

$$I(q) = n \left[\frac{3V_{tot}(\Delta\rho)[\sin(qR) - qR \cos(qR)]}{(qR)^3} \right]^2 S(q) \quad (S8)$$

where R is the particle radius and $\Delta\rho$ is the scattering length density difference of the particle and the solvent.

Except for the pure P65 and F127 solutions ($MR = 0$) at 20 °C where no polydispersity was used, the polydispersities of the R_{core} , R and the shell thickness, d_{shell} (defined as $d_{shell} = R_{tot} - R_{core}$) for all mixture were described by Schultz distribution as following

$$f(x) = \frac{x^2}{Norm \cdot PD^{z+1}} \left[\frac{x}{x_{mean}} \right]^{z+1} \exp \left[- (z + 1) \frac{x}{x_{mean}} \right] \quad (S9)$$

where $Norm$ is the normalization factor, x_{mean} is the mean of the distribution, $Z = 1/PD^2 - 1$. PD is the polydispersity defined as $PD = \sigma/x_{mean}$ and $\sigma = w/\sqrt{3}$, where w is the half width.

The mixed F127—NaGDC solutions at $MR = 0-12$ at 50 °C were only treated with the Bayesapp software. The core-shell form factor was not appropriate to use in this case and a more advanced model was needed as presented by Pedersen et al.¹⁵ However, since the Bayesapp fits of the P65—NaGDC mixed system corresponded well with the fits using the core-shell form factor and HP structure factor, we utilized the Bayesapp fitting results in the comparisons between the different block copolymer systems.

REFERENCES

1. Hvidt, S.; Jørgensen, E. B.; Brown, W.; Schillén, K., Micellization and Gelation of Aqueous Solutions of a Triblock Copolymer Studied by Rheological Techniques and Scanning Calorimetry. *J. Phys. Chem.* **1994**, *98*, 12320-12328.
2. Hvidt, S.; Trandum, C.; Batsberg, W., Effects of Poloxamer Polydispersity on Micellization in Water. *Macromolecules* **2004**, *250*, 2965-2971.
3. Bayati, S.; Galantini, L.; Knudsen, K. D.; Schillén, K., Effects of Bile Salt Sodium Glycodeoxycholate on the Self-Assembly of PEO-PPO-PEO Triblock Copolymer P123 in Aqueous Solution. *Langmuir* **2015**, *31*, 13519-13527.
4. Löf, D.; Niemiec, A.; Schillén, K.; Loh, W.; Olofsson, G., A Calorimetry and Light Scattering Study of the Formation and Shape Transition of Mixed Micelles of EO₂₀PO₆₈EO₂₀ Triblock Copolymer (P123) and Nonionic Surfactant (C₁₂EO₆). *J. Phys. Chem. B* **2007**, *111*, 5911-5920.
5. Janiak, J.; Bayati, S.; Galantini, L.; Pavel, N. V.; Schillén, K., Nanoparticles with a Bicontinuous Cubic Internal Structure Formed by Cationic and Non-Ionic Surfactants and an Anionic Polyelectrolyte. *Langmuir* **2012**, *28*, 16536–16546.
6. Jakeš, J., Regularized Positive Exponential Sum (REPES) Program—A Way of Inverting Laplace Transform Data obtained by Dynamic Light Scattering. *Collect. Czech. Chem. Comm.* **1995**, *60*, 1781-1797.
7. Schillén, K.; Brown, W.; Johnsen, R. M., Micellar Sphere-to-Rod Transition in an Aqueous Triblock Copolymer System. A Dynamic Light Scattering Study of Translational and Rotational Diffusion. *Macromolecules* **1994**, *27*, 4825-4832.

8. Stepanek, P., Data Analysis in Dynamic Light Scattering. In *Dynamic Light Scattering: The Method and Some Applications*, Brown, W., Ed. Oxford University Press: Oxford, 1993; pp 177-241.
9. Hansen, S., Simultaneous Estimation of the Form Factor and Structure Factor for Globular Particles in Small-Angle Scattering. *J. Appl. Cryst.* **2008**, *41*, 436-445.
10. SasView for Small Angle Scattering Analysis, <http://www.sasview.org/>.
11. Percus, J. K.; Yevick, G. J., Analysis of Classical Statistical Mechanics by means of Collective Coordinates. *Phys. Rev.* **1958**, *110*, 1-13.
12. Kinning, D. J.; Thomas, E. L., Hard-Sphere Interactions between Spherical Domains in Diblock Copolymers. *Macromolecules* **1984**, *17*, 1712-1718.
13. Hayter, J. H.; Penfold, J., An Analytic Structure Factor for Macroion Solutions. *Mol. Phys.* **1981**, *42*, 109-118.
14. Manet, S.; Lecchi, A.; Imperor-Clerc, M.; Zholobenko, V.; Durand, D.; Oliveira, C. L. P.; Pedersen, J. S.; Grillo, I.; Meneau, F.; Rochas, C., Structure of Micelles of a Nonionic Block Copolymer Determined by SANS and SAXS. **2011**, *115*, 11318–11329.
15. Pedersen, J. S.; Gerstenberg, M. C., Scattering Form Factor of Block Copolymer Micelles. *Macromolecules* **1996**, *29*, 1363-1365.